

Supplementary figure legends:

Figure S1: FcγR binding of RTX and tetra-Fc-sialylated RTX. Binding of RTX and tetra-Fc-sialylated RTX to CHO cells either untransfected or transfected with the indicated FcγRs analyzed by flow cytometry. (RTX, Rituximab; CHO, Chinese hamster ovary cells; His, Histidine; Arg, Arginine)

Figure S2. Schematic representation of antibody glycan modification. (A) Scheme showing the major processing steps yielding the various antibody glycovariants. (B) Schematic depiction of a tetra-Fc-sialylated IgG carrying two G2SA2 glycans and relative abundance of individual IgG-Fc glycans in the antibody glycovariants. (β1,4GalT, β1-4 galactosyltransferase-1; ST6Gal, α2,6-sialyltransferase; N297, Asparagine 297; Endo-S, Endoglycosidase S)

Figure S3. RTX and hu8-18C5 N-glycosylation sites. (A) Amino acid sequence of RTX and hu8-18C5 heavy chain (HC) and light chain (LC) were analyzed for potential N-glycosylation sites. Both antibodies only contain the conserved Fc-N-glycosylation site at asparagine 297 (N297, depicted in bold) and no glycosylation sites in the HC and LC variable regions. N-glycosylation sites (Asn-Xaa-Ser/Thr) were identified using the NetNGlyc 1.0 server from the Technical University of

Denmark (DTU). RTX sequences were obtained from www.drugbank.ca (Acc. Nr. DB00073) and hu8-18C5 sequences were translated from the expression plasmids.

(B) Acrylamide gel electrophoresis of RTX and hu8-18C5. Silver staining (left) and Immunoblotting using the mannose-specific lectin *Lens culinaris* agglutinin (right). (RTX, Rituximab; HC, heavy chain; LC, light chain)

Figure S4. IgG-Fc sialylation reduces C3b deposition. C3b deposition to Raji cells in the presence or absence of 10 µg/ml RTX or glycovariants of RTX analyzed by flow cytometry **(A)** and quantification of C3b deposition after 30 minutes **(B)** Mean and SD of 3 independent experiments. For inter-assay normalization the median fluorescence intensity signal obtained for the unmodified antibody after 60 min was set to 100 and the relative signal was calculated for all other data points; Statistics were performed by 1-way ANOVA and Bonferroni post test. (RTX, Rituximab)

Figure S5: Serum IgG content in CIDP patients and IgG-Fc glycosylation in IVIG treated patients included in the ICE trial. Serum IgG content was measured by ELISA. Relative IgG content compared to study entry is shown. **(A)** Serum of CIDP patients participating in the ICE trial was taken before and 2 weeks after the last treatment with IVIG (right) or placebo (left) **(B)** Patients from an independent cohort (“Marburg cohort”) all received IVIG. Serum was taken 3-5 weeks following the last infusion of IVIG (mean +/- SD: 4.0 +/- 0.6). Statistics were performed by Wilcoxon matched pairs test. (IVIG, intravenous immunoglobulin) **(C)** Serum IgG-Fc glycan composition of IVIG treated CIDP patients from the ICE cohort analyzed by lectin blotting. Relative frequencies of IgG-Fc glycoforms in CIDP patients before and after 24 weeks of IVIG therapy. Patients received IVIG infusions every 3 weeks for up to

24 weeks and samples were taken 2 weeks after the last infusion. Patients with disease remission upon IVIG therapy are compared to those with stable or worsening disease (no remission). The increase in total IgG serum levels 2 weeks after the last infusion precluded profiling of endogenous IgG in this cohort. Statistics were performed by Mann-Whitney U test.

Table S1. Patients' Characteristics.

Table S1

Number of patients	33	
Age at study entry (Median; range)	62; 32 - 79	
Duration of symptoms (years)	< 1 - 15	
Male to female ratio	22:11	
Fulfilling modified AAN criteria	94%	
Fulfilling EFNS/PNS criteria	100%	
Clinical course	number of patients	% of patients
Relapsing-remitting	5	15.1
Primary progressive	26	78.8
Monophasic	2	6.1
CIDP subtype		
CIDP	25	75.8
CIDP-MGUS	0	0
DADS	3	9.1
MADSAM	5	15.2
Treatment response	31	94

Figure S1

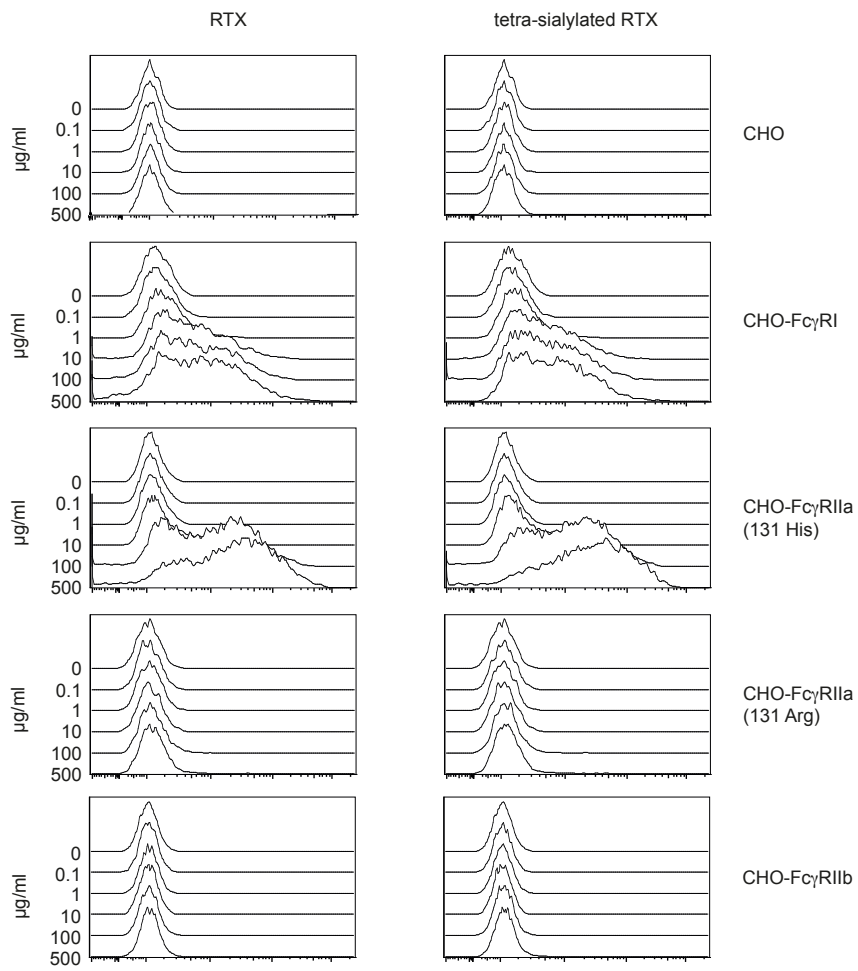
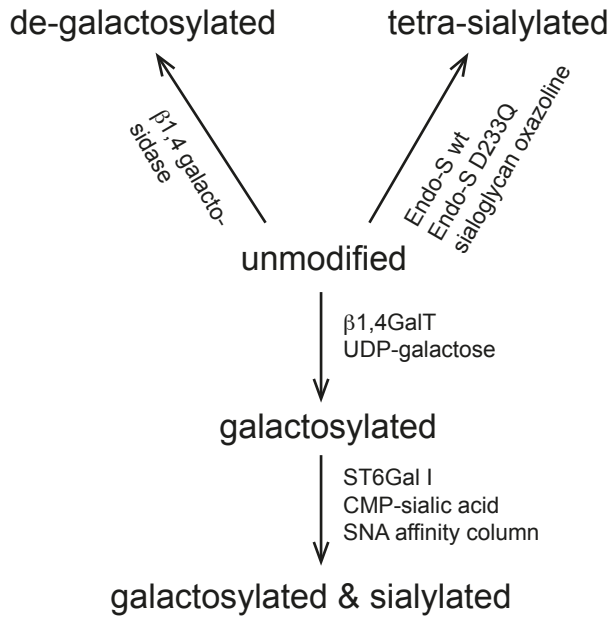


Figure S2

A



B

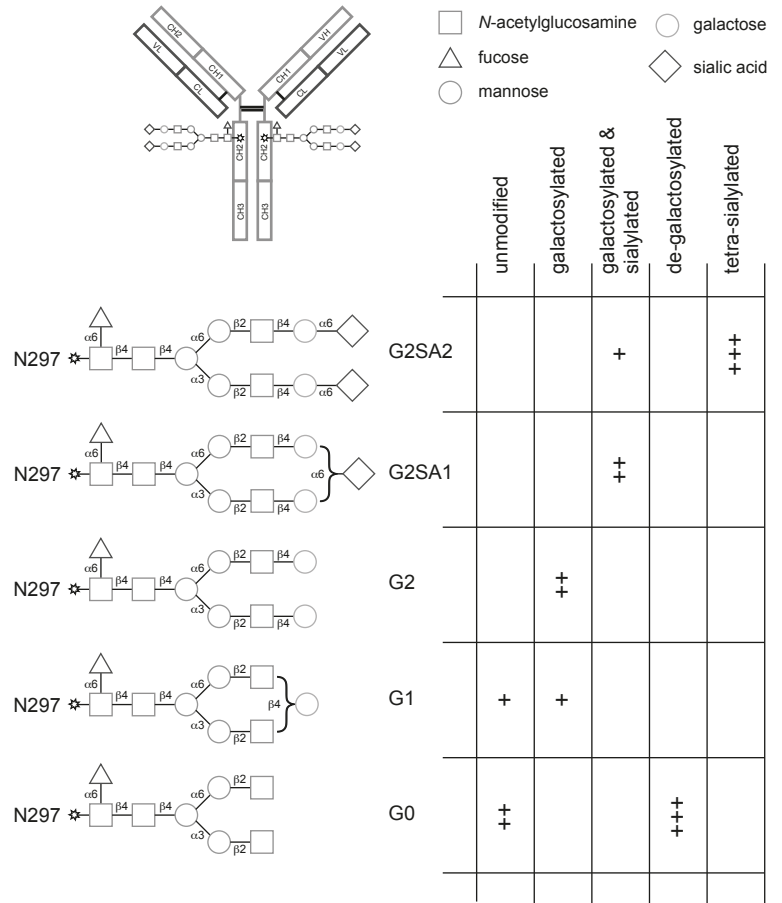


Figure S3

A

RTX HC

```

QVQLQQPGAELVKPGASVKMSCKASGYFTSYNMHWVKQTPGRGLEWIGAIYPNGDTSYNQKFKGKATLTADKSSSTAY 80
MQLSSLTSEDSAVYYCARSTYYGGDWYFNWVGAGTTVTVAASTKGPSVFPLAPSSKSTSGGTAALGCLVKDYFPEPVTV 160
SWNSGALTSQVHTFPAVLQSSGLYSLSSVTVPSSSLGTQTYICNVNHKPSNTKVDKVEPKSCDKTHTCPPCPAPELLG 240
GPSVFLFPPKPKDTLMISRTPEVTCVVDVSHEDPEVKFNWYVDGVEVHNAKTKPREEQYNSTYRVVSVLTVLHQDWLNG
KEYKCKVSNKALPAPIEKTISKAKGQPREPQVYTLPPSRDELTKNQVSLTCLVKGFYPSDIAVEWESNGQPENNYKTTTP 320
VLDSGGSFFLYSKLTVDKSRWQQGNVFCFSVMHEALHNHYTQKLSLSPGK 400
    
```

RTX LC

```

QIVLSQSPAILSASPGEKVTMTCRASSSVYIHWFOQKPGSSPKPWIIYATSNLASGVPVRFSGSGSGTSYSLTISRVEAE 80
DAATYYCQOWTNSNPTFTGGGKLEIKRTVAAPSVFIFPPSDEQLKSGTASVCLLNNFYPREAKVQWKVDNALQSGNSQE 160
SVTEQDSKDYSLSSSTLTLKADYEKHKVYACEVTHQGLSSPVTKSFNRGEC
    
```

hu8-18C5 HC

```

QVQLQQSGAELMKPGASVEISCKATGYTFSSFWIEWKQRPQGHLEWIGELPGRGRNTNYNEFKGKATFTAETSSNTAY 80
MQLSSLTSEDSAVYYCATGNTMVMNIPYWGQGTTLTVSSASTKGPSVFPLAPSSKSTSGGTAALGCLVKDYFPEPVTVSWN 160
SGALTSQVHTFPAVLQSSGLYSLSSVTVPSSSWHPTYICNVNHKPSNTKVDKREPKSCDKTHTCPPCPAPELLGGPSV
FLFPPKPKDTLMISRTPEVTCVVDVSHEDPEVKFNWYVDGVEVHNAKTKPREEQYNSTYRVVSVLTVLHQDWLNGKEYK 320
CKVSNKALPAPIEKTISKAKGQPREPQVYTLPPSREEMTKNQVSLTCLVKGFYPSDIAVEWESNGQPENNYKTTTPVLD 400
DGSFFLYSKLTVDKSRWQQGNVFCFSVMHEALHNHYTQKLSLSPGK
    
```

hu8-18C5 LC

```

DIELTQSPSSLAVSAGEKVTMSCKSSQSLNSGNQKNYLAWYQQKPLPKLLIYGASTRESGVPDRFTGSGSGDFTLT 80
ISSVQAEALAVYYCQNDHSYPLTFGAGTKLEIKRTVAAPSVFIFPPSDEQLKSGTASVCLLNNFYPREAKVQWKVDNAL 160
QSGNSQESVTEQDSKDYSLSSSTLTLKADYEKHKVYACEVTHQGLSSPVTKSFNRGEC
    
```

B

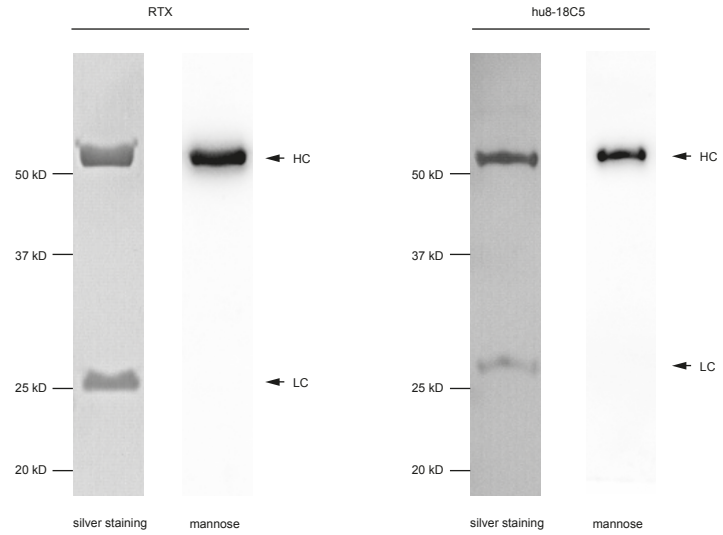
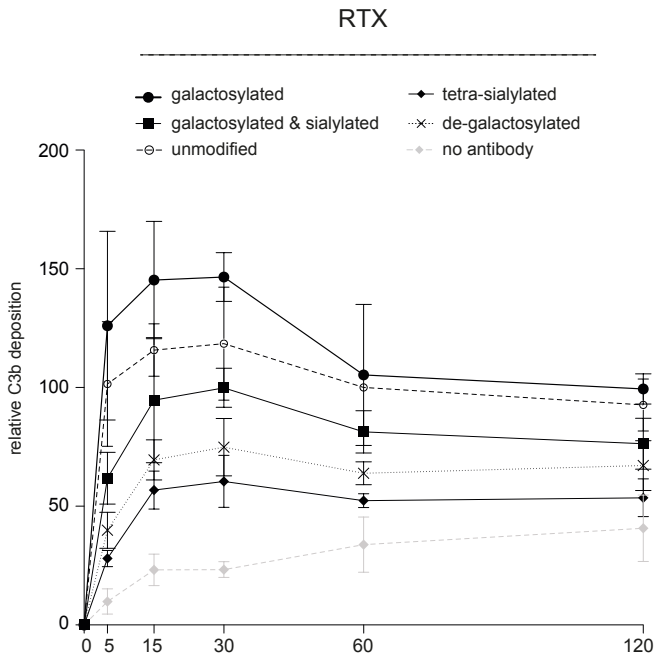


Figure S4

A



B

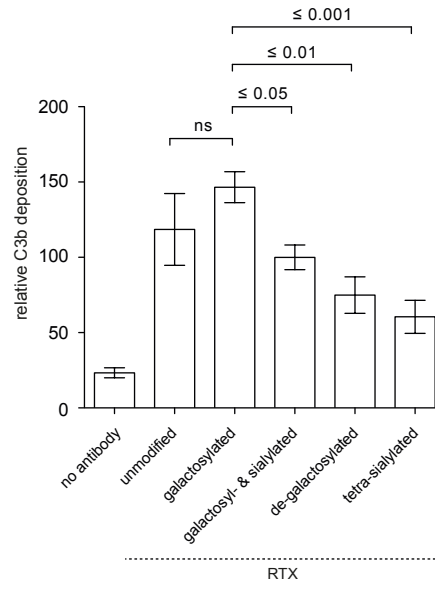
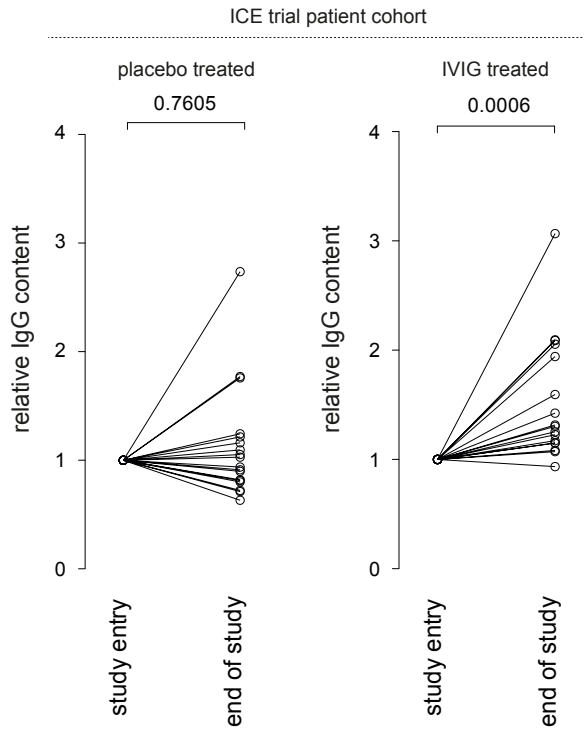
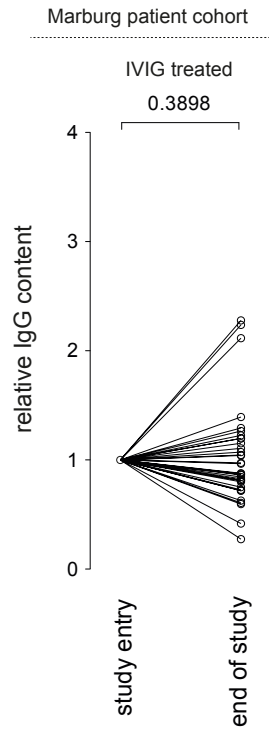


Figure S5

A



B



C

